

Electronic Supplementary Information of

Seeds screening aqueous synthesis, multiphase
interfacial separation and *in-situ* optical
characterization of invisible ultrathin silver nanowires

Xiao-Yang Zhang^{a, b, c}, Xiao-Mei Xue^b, Huan-Li Zhou^a, Ning Zhao^{a, b, c}, Feng Shan^{a, c}, Dan Su^{b, c},

Yi-Ran Liu^a and Tong Zhang^{*a, b, c}

^a *Joint International Research Laboratory of Information Display and Visualization, School of Electronic Science and Engineering, Southeast University, Nanjing, 210096, People's Republic of China.*

^b *Key Laboratory of Micro-Inertial Instrument and Advanced Navigation Technology, Ministry of Education, and School of Instrument Science and Engineering, Southeast University, Nanjing, 210096, People's Republic of China.*

^c *Suzhou Key Laboratory of Metal Nano-Optoelectronic Technology, Suzhou Research Institute of Southeast University, Suzhou, 215123, People's Republic of China.*

Corresponding Author

*Email: tzhang@seu.edu.cn

1. SEM images of samples synthesized under different reaction conditions

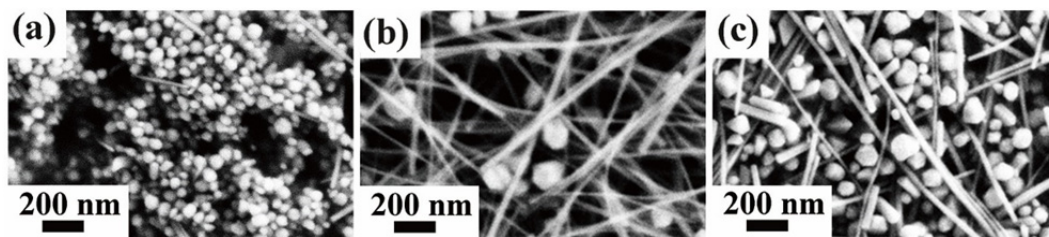


Fig. S1 SEM images of samples synthesized with different light exposure times from 0 min in (a), 10 min in (b), to 2 h in (c), respectively.

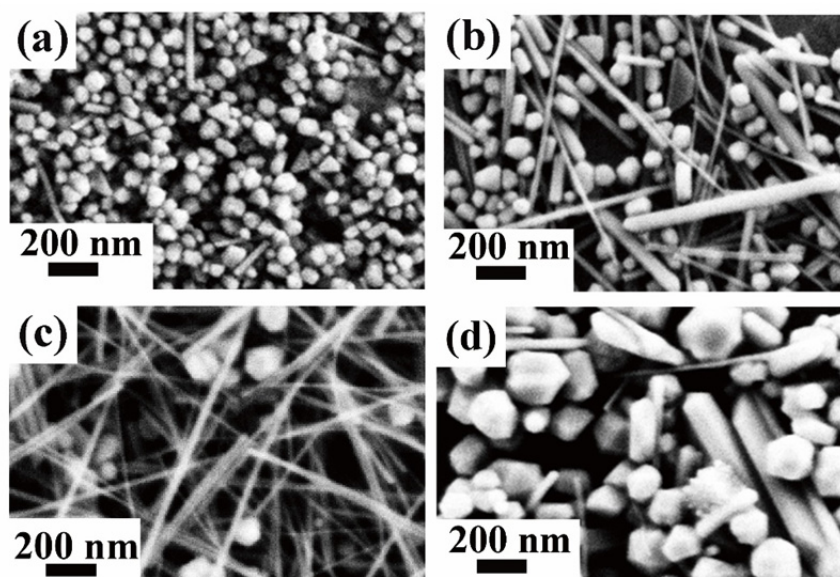


Fig. S2 SEM images of samples synthesized by adding different amounts of H_2O_2 from 0 mL in (a), 0.2 mL in (b), 0.6 mL in (c), to 1.2 mL in (d), respectively.

2. Investigation of the molecular weight of PVP in the synthesis process

We also investigated the importance of molecular weight of PVP used in our proposed method. During the synthesis process, any other conditions including the amount of PVP added were kept the same, only the molecular weight of PVP was changed. PVP with three different molecular weight from 8 K, 55 K to 1300 K were used in the comparison experiments, separately. The extinction spectra of the final synthesized samples were measured and shown in Figure S3. As identified from the specific LSPR bands in the curves, the final obtained silver nanostructures were quite different although the amounts of PVP used were the same. When PVP with molecular weight

of 8 K or 55 K was used, silver nanospheres with a single LSPR band distributing at ~ 450 nm were the primary products. The broaden LSPR band covering the range from 400 nm to 700 nm further reflected the size irregularity of the silver nanospheres. Only when ultra-long molecular chain PVP (molecular weight of 1300 K) was used, high yield of silver nanowires can be obtained.

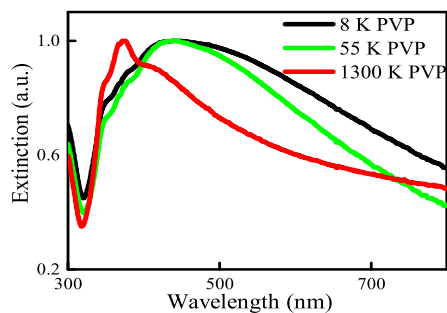


Fig. S3 Extinction spectra of silver nanostructure samples synthesized using PVP with different molecular weights

3. Feature comparison of different synthesis and purification methods of silver nanowires

Here we compared the specific features of previously reported synthesis and purification strategies^[1-6] and our proposed method, as listed in Table S1. The comparison was focused on the following four aspects including solvent used, specific reaction condition, diameter control of the synthesized silver nanowires, and newly proposed purification methods. As shown in the table, ethylene glycol is the most popular candidate used as a solvent as well as a weak reducer for silver nanowire synthesis. However, the reflux of ethylene glycol and the following reducing process usually require high temperature environment at least over 150 °C. The diameter of silver nanowires synthesized in ethylene glycol solvent primarily distributes in the range of 40-150 nm^[1-3]. After the continuous efforts of researchers, silver nanowires with diameter ranged in the level of ~ 20 nm have been achieved near recently^[5-6]. However, to keep the synthesized silver nanowires thin enough, rigorous reaction conditions such as extremely high pressure (up to 1000 psi corresponding to ~ 68 folds of standard atmospheric pressure) and N₂ gas protection are usually required. There are only a few papers reporting the synthesis strategy of silver nanowires in aqueous environment^[4]. Silver nanowires with mean diameter of 33 nm were synthesized in water. However, rigorous reaction condition such as high temperature (40 °C over the Boiling point of water) and N₂ gas protection were also required. In comparison, our proposed method is superior in diameter control and reaction cost saving. Silver nanowires with a mean diameter down to 16 nm have been successfully achieved

by our method at a relative low temperature ($\sim 90^\circ\text{C}$) and conventional atmospheric environment. More importantly, silver nanowires with diameter as thin as 8 nm can be easily observed in our samples. To the best of our knowledge, it is the first time that a synthesis method of silver nanowires with sub-10 nm was reported. Furthermore, compared to organic solvent such as ethylene glycol, water used in our method is a quite low-cost and environment friendly solvent meeting the future requirement of industrialization.

The purification of silver nanowires is also very important for practical applications. As seen from Table S1, several purification strategies have been proposed to purify the as-synthesized silver nanowires. However, different purification strategies may be only suitable for purification of silver nanowires with specific morphologic features. For our method synthesized silver nanowires, it was quite difficult to purify by previously reported methods which have been verified by a series of trial experiments. It is because such type of crystal structures is ultrathin, light weight and soft. Fortunately, our proposed two-phase purification approach can be used to separate such thin silver nanowires from various by-products with different morphologies effectively by surface energy identification.

Table S1 Comparison of silver nanowire synthesis and purification methods

Ref.	Solvent	Specific reaction condition	Diameter of nanowires	New purification method proposed
1	Ethylene glycol	151 $^\circ\text{C}$	100-150 nm	-
2	Ethylene glycol	170 $^\circ\text{C}$	80 nm	Yes
3	Ethylene glycol	160 $^\circ\text{C}$	40-80 nm	Yes
4	Water	140 $^\circ\text{C}$ + high-pressure	33 \pm 2 nm	-
5	Ethylene glycol	170 $^\circ\text{C}$ +N ₂	20 \pm 2 nm	Yes
6	Ethylene glycol	High-pressure + N ₂	20nm	-
This work	Water	Seed screening by short time LED irradiation at 90 $^\circ\text{C}$ + H ₂ O ₂	8-20 nm	Yes

In order to explain the role of TBAB in the purification of Ag NWs, we executed the in-situ energy dispersive spectrometer (EDS) measurement of single Ag NW and particle under the TEM observation as shown in Figure S4 and S5. Note that for the TEM and EDS measurement in Figure S., as the silver nanostructures samples were prepared on the TEM Cu meshwork supporting carbon film, Cu peak existed and cannot be eliminated in the EDS results.

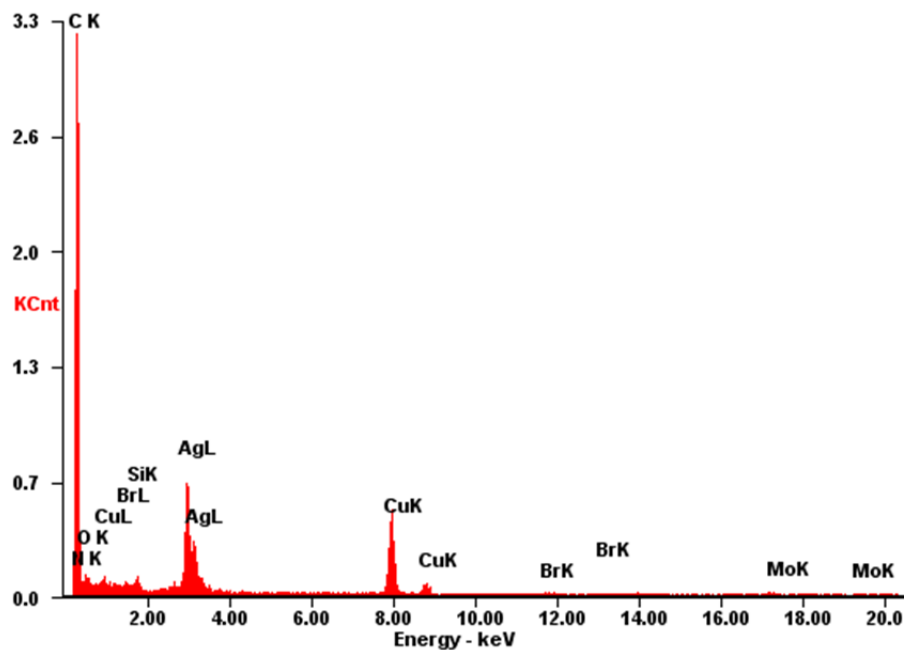


Fig. S4 EDS of a single AgNW

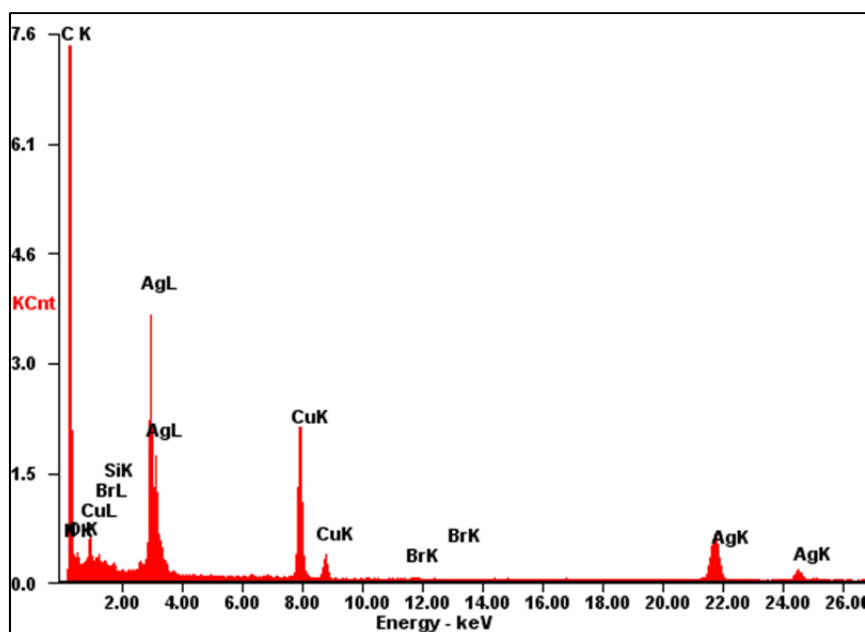


Fig. S5 EDS of a single silver nanoparticle

4. Illustration of in-situ tracking of silver nanowires

In this experiment, the diameter of the silver nanowires was taken from the high resolution SEM images. The optical characteristics of the silver nanowires were analyzed by multi-functional approaches under the Olympus IX-71 optical microscope. To identify single silver nanowire with a certain diameter from massive nanostructures located on the surface of substrate and record its

optical images, absorption spectrum and the morphology by different equipments, the effective in-situ tracking approach is necessary. Here we used bared TEM copper mesh to mark the position of the samples generally. The accurate position of single nanowires were then be identified by the specific distribution of the adjacent nanostructures such as nanospheres and short nanorods which interact with visible light strongly, as illustrated in Figure S6 and Figure S7. It is evident that these silver nanowires can be easily identified both in SEM and optical microscope images.

For sample preparation of silver nanowires with different diameters, different synthesis methods were used. Ultrathin silver nanowires were prepared by our proposed method, as shown in Figure S6. To enhance the identification efficiency, small silver nanospheres served as specific markers were also added as discussed above. The accurate position of a single silver nanowire with a diameter of 15 nm can be clearly identified in these images. Conventional polyol process was used to synthesis thicker silver nanowires for comparison. Figure S7 showed the synthesized silver nanowires using conventional polyol process without carefully controlling of diameter. Silver nanowires with diameter distributing from several tens of nanometers to over 200 nanometers can be found in Figure S7 clearly.

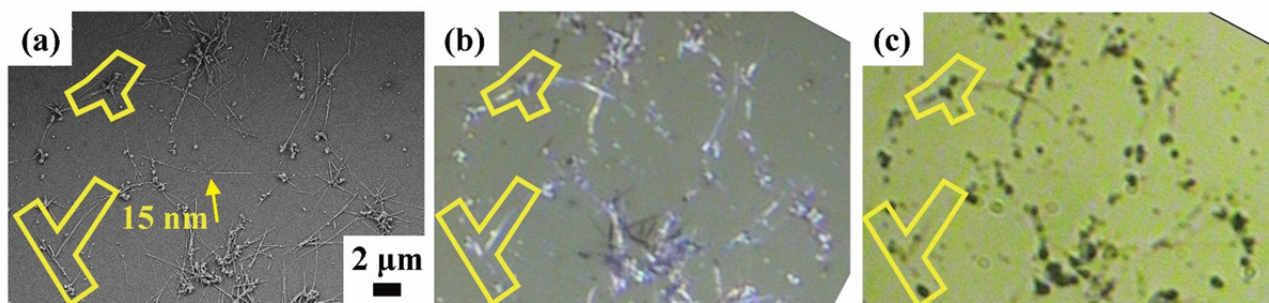


Fig. S6 In-situ comparison of morphologic and optical imaging of the silver nanowires with diameter of 15 nm. (a) SEM image, (b) optical microscopic image by reflected light path, and (c) optical microscopic image by transmitted light path. The specific patterns in yellow color illustrate the one-to one match features in these three images.

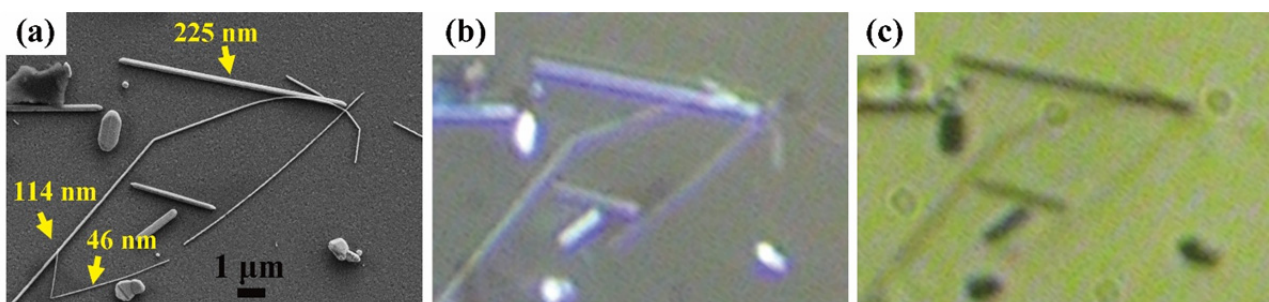


Fig. S7 In-situ comparison of morphologic and optical imaging of the silver nanowires with diameter of 46 nm, 114 nm and 225 nm. (a) SEM image, (b) optical microscopic image by reflected light path, and (c) optical microscopic image by transmitted light path.

5. Imaging strategy illustration of silver nanowires by white light illumination

The imaging strategies of silver nanowires under the illumination of white LED by reflected light path and transmitted light path are shown in Figure S8 (a) and (b), respectively. Olympus IX-71 optical confocal microscope was used to image the silver nanowires. The positions of the ITO glass substrate, silver nanowire, 100× microscopic lens, 50% light beam splitting mirror, and CCD in these two imaging strategy are the same. The only difference is the illumination direction of the light source. As shown in Figure S8 (a), white LED was placed at the left of the 50% light beam splitting mirror. Using this strategy, the CCD recorded the backscattering light behavior of silver nanowires under the illumination of white light. In comparison, when white LED was placed at the other side of ITO glass substrate, the CCD recorded the white light image after light passed through the silver nanowires, as illustrated in Figure S8 (b)

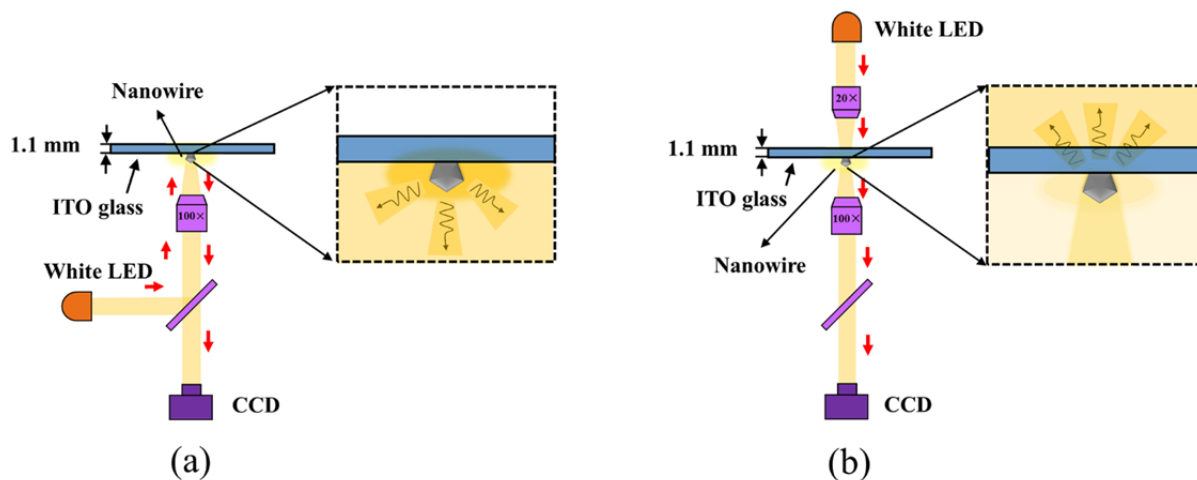


Fig. S8 Schematic illustrations of silver nanowire imaging by (a) reflected light path and (b) transmitted light path.

6. Imaging strategy illustration of silver nanowires by focused laser beam with mono-wavelength

The imaging strategy of silver nanowires under the illumination of focused laser beam with mono-wavelength is illustrated in Figure S9. Supercontinuum white laser source (SC-PRO, 6W, Yangtze Soton Laser Co., Ltd., China) first passed through an acousto-optic tunable filter system (AOTF-Pro, Yangtze Soton Laser Co., Ltd., China). Aligned mono-wavelength laser with a

bandwidth of ~ 10 nm was obtained. The central wavelength peak of the laser beam can be tuned easily in the range between 450 nm and 700 nm by acousto-optic effect. Then the laser beam was focused to be a light spot at the level of optical diffractive limit by a $100\times$ microscope lens, right on the surface of single silver nanowire for optical imaging. As illustrated in Figure S9, the image directly reflected the backscattering behavior of silver nanowires under the illumination of mono-wavelength laser beam.

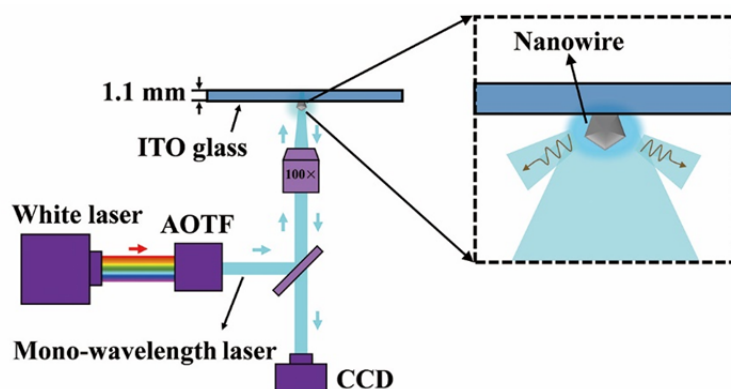


Fig. S9 Schematic illustrations of silver nanowire imaging by focused laser beam with mono-wavelength.

7. Investigation of the relationship between optical characteristics and morphological feature of silver nanowire film by in-situ imaging and spectroscopic measurement

Figure S10 compared the electric field distributions of AgNWs of 3D modeling using different configurations. For practical fabrication of AgNWs based TCFs, the AgNWs are placed on glass substrate as shown in Figure S10 (b). Comparing with the simulation result for AgNW surrounded by air (Figure S10 (a)), when AgNW is placed on glass substrate, forward light scattering becomes more obvious. Considering the in-situ optical measurement of AgNWs was obtained using conductive ITO glass as substrates, we also provided the simulation result for AgNW placed on ITO glass (Figure S10 (c)) similar to the configuration used in our in-situ optical measurement. The compared result indicated the simulated electric-field distributions shown in Figures S10 (b) and (c) are principally the same. It indicated that the experimental result obtained from our in-situ optical measurement of Ag NWs and feature structures in AgNW based film can effectively show similar optical characteristics of AgNWs on glass substrates which conventionally used in AgNW based TCFs.



Fig. S10 3D simulation of electric-field distribution of AgNWs in air (a), located on glass substrate without (b) or with a layer of ITO seen from the cross-sectional view.

For AgNWs with diameter increasing to 225 nm, multiple plasmonic modes with different N_{eff} can be supported as shown in Figure S11. Therefore light scattering become much more complicate for such thick AgNWs.

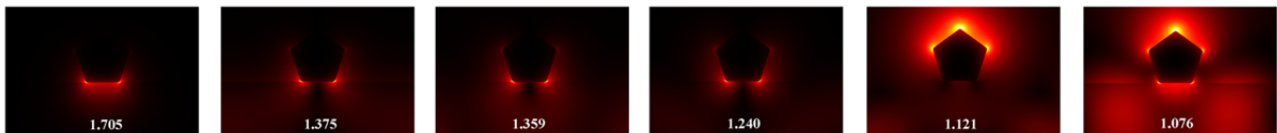


Fig. S11 Electric-field distribution of plasmonic modes supported by AgNWs with a diameter of 225 nm located on the glass substrate. N_{eff} of these modes were recorded at the bottom of the figures.

Figure S12 to Figure S14 provided large-scale optical and SEM images of our in-situ optical measurement experiment, illustrating how we identify and effectively obtain optical images, SEM images and micro-domain optical spectra of various AgNW feature structures in-situ.

Typical feature structures obtained from silver meshwork using conventional fabrication process were illustrated by yellow arrows in high resolution SEM images in Figure S12 (e) to (g). It is clearly showed in Figure S12 (e) that the joint of cross AgNWs is much thicker than separated AgNWs after sintering treatment. Therefore, light scattering becomes much more obvious at these nodes. Cross lines with different angles as shown in Figure S12 (f) and randomly aggregated AgNWs as shown in Figure S12 (g) can not be avoid using conventional fabrication processes and undoubtedly further enlarge the light scattering behavior of AgNW film.

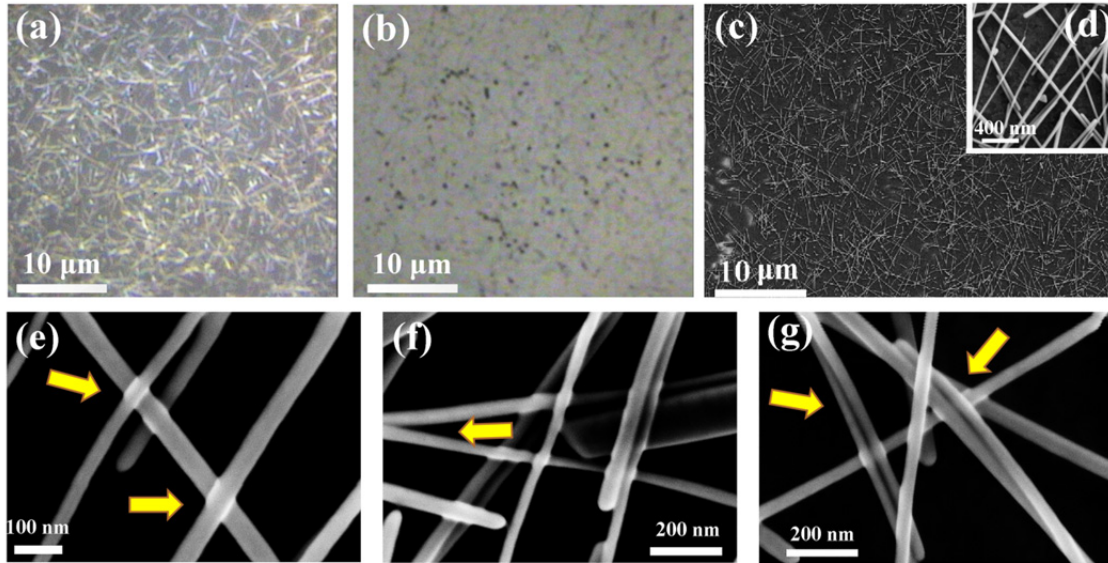


Fig. S12 In-situ comparison of AgNWs film imaged by (a) reflected light path and (b) transmitted light path. (c) shows the SEM of silver nanowire film. (d) shows the detailed distribution of silver nanowire film. (e) to (g) show the high resolution SEM images containing the general morphological features of the deposited silver nanowires.

In Figure S13, three arrows with different colors illustrated a single AgNW, a node of cross line and an AgNW dimer with ~ 200 nm gap distance at the same field of view. It is clearly shown that even for thin AgNWs which diameter is only 30-45 nm, the back scattering of these nanowires are still obvious. More important, it is unexpected that we observed the back scattering shown in Figure S13 (a) and transmission decrease shown in Figure S13 (b) for AgNW dimer with ~ 200 nm gap distance is much more obvious than that of single AgNW and node of cross AgNW.

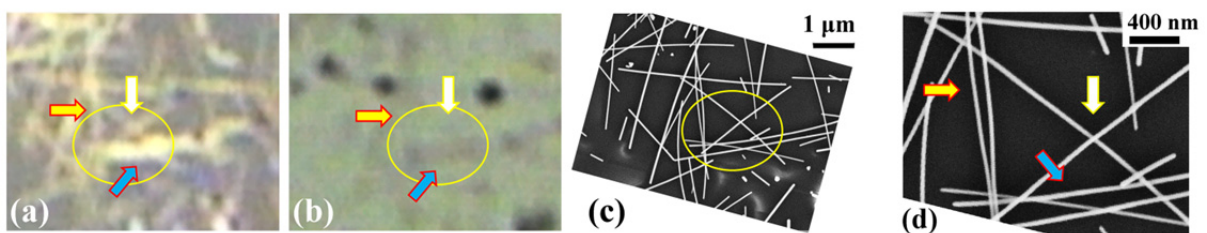


Fig. S13 In-situ comparison of the magnified images of silver film constituted by silver nanowires with diameter between 30 nm to 45 nm synthesized by conventional polyol process. (a), (b) and (c) compared the general optical image of reflected light path, transmitted light path and SEM of the silver film in-situ. (d) shows the high resolution image using for morphological feature and diameter identification.

In comparison, the back scattering as shown in Figure 14 (a) is very weak for ultrathin AgNW film. Even for these nanowire bundles containing several aggregated AgNWs as illustrated by yellow and red arrows, the back scattering of light is still much weaker than that of AgNWs in

Figure S13. Furthermore, Figure S14 (b) clearly show the transmission light across the ultrathin AgNW film is nearly 100%. From the comparison above, one can see clearly that AgNW film with low haze and high transparency can be easily obtained using ultrathin AgNWs. It is a big improvement for TCF fabrication.

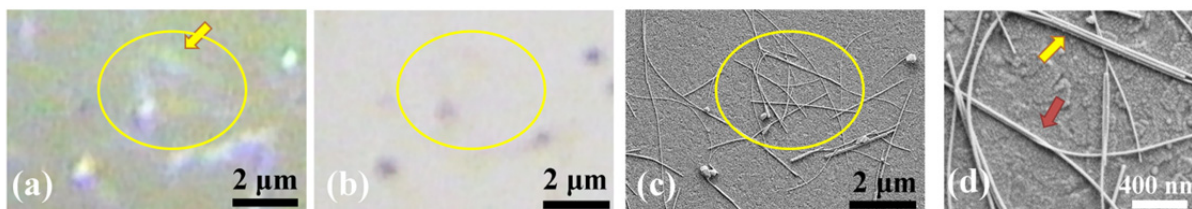


Fig. S14 In-situ comparison of the magnified images of silver film constituted by ultrathin silver nanowires with diameter thinner than 20 nm synthesized by currently proposed aqueous method. (a), (b) and (c) compared the general optical image of reflected light path, transmitted light path and SEM of the silver film in-situ. (d) shows the high resolution image using for morphological feature and diameter identification.

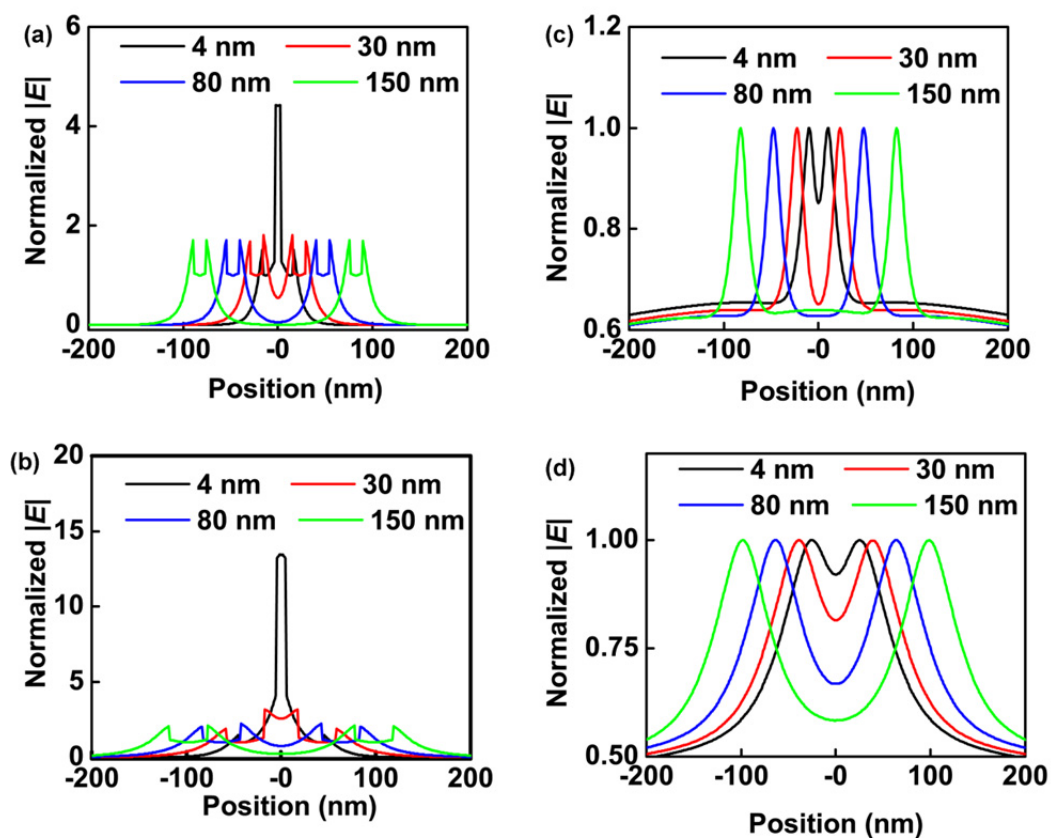


Fig. S15 Profiles of the normalized electric-field distribution taken from the positions (labeled by blue dish lines in Figure 12) of bound mode patterns (in (a) and (b)), and leaky mode patterns (in (c) and (d)), respectively. Diameter of

AgNWs is 15 nm in (a) and (c) and 46 nm in (b) and (d), respectively.

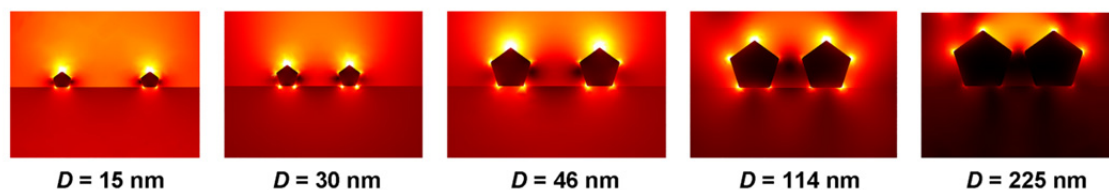


Fig. S16 3D simulation of electric-field distribution of AgNW dimer with a distance of 60 nm and different diameters seen from the cross-sectional view.



Fig. S17 Experimental setting of the LED illumination step seen from different view angles.

References:

- [1] Lee, P.; Lee, J.; Lee, H.; et al. Highly Stretchable and Highly Conductive Metal Electrode by Very Long Metal Nanowire Percolation Network. *Advanced Materials* **2012**, *24*, 3326–3332.
- [2] Pradel, K. C.; Sohn, K.; Huang, J. Cross-Flow Purification of Nanowires. *Angewandte Chemie International Edition* **2011**, *50*, 3412–3416.
- [3] Mayousse, C.; Celle, C.; Moreau, E.; et al. Improvements in Purification of Silver Nanowires by Decantation and Fabrication of Flexible Transparent Electrodes. Application to Capacitive Touch Sensors. *Nanotechnology* **2013**, *24*, 215501.
- [4] Wang, C.; Cheng, B.; Zhang, H.; et al. Probing the Seeded Protocol for High-Concentration Preparation of Silver Nanowires. *Nano Research* **2016**, *9*, 1532–1542.

[5] Li, B.; Ye, S.; Stewart, I. E.; et al. Synthesis and Purification of Silver Nanowires to Make Conducting Films with a Transmittance of 99%. *Nano letters* **2015**, *15*, 6722–6726.

[6] Lee, E. J.; Kim, Y. H.; Hwang, D. K.; et al. Synthesis and Optoelectronic Characteristics of 20 nm Diameter Silver Nanowires for Highly Transparent Electrode Films. *RSC Advances* **2016**, *6*, 11702–11710.